Systems Science and Informatics Unit (SSIU)
Indian Statistical Institute, Bangalore
India

ESIEE
University of Paris-Est
France

19-22 October 2010
Bangalore

TERRESTRIAL ANALYSIS
PART-II

1

ANALYSES OF COMPLEX TOPOLOGICAL AND SURFICIAL FEATURES RETRIEVED FROM DIGITAL ELEVATION MODELS (DEMs) AND SPATIAL MAPS

B. S. Daya Sagar

Outline

- Introduction
- Objectives
- Study area specification
- Results
- Conclusions
- Future Recommendations
- Mathematical Morphological Transformations employed in this part include: Morphological Shape Decomposition, Granulometries, Half-Plane Closings to generate Convexhulls, Geodesic Dilations

3

Introduction

- The two major phases involved in analyzing the spatial and topological information from remotely sensed and topographic data include
- (a) extraction of features from DEMs.
- (b) generation of non network space from network.
- Several algorithms have been proposed to extract features from DEMs.

4

Objectives

♦ To propose morphology based method via fragmentation rules to compute scale invariant but shape-dependent measures of non-network space of a basin.

♦ To make comparisons between morphometry based parameters / dimensions and dimensions derived for non-network space.

5

Derivation of maps from remotely sensed and topographic data sources – Phase II

♦ **Data Used:** Following illustration shows SPOT X band data of Machap Baru reservoir catchment.

♦ Following figure illustrates the mapped features within this catchment.

6

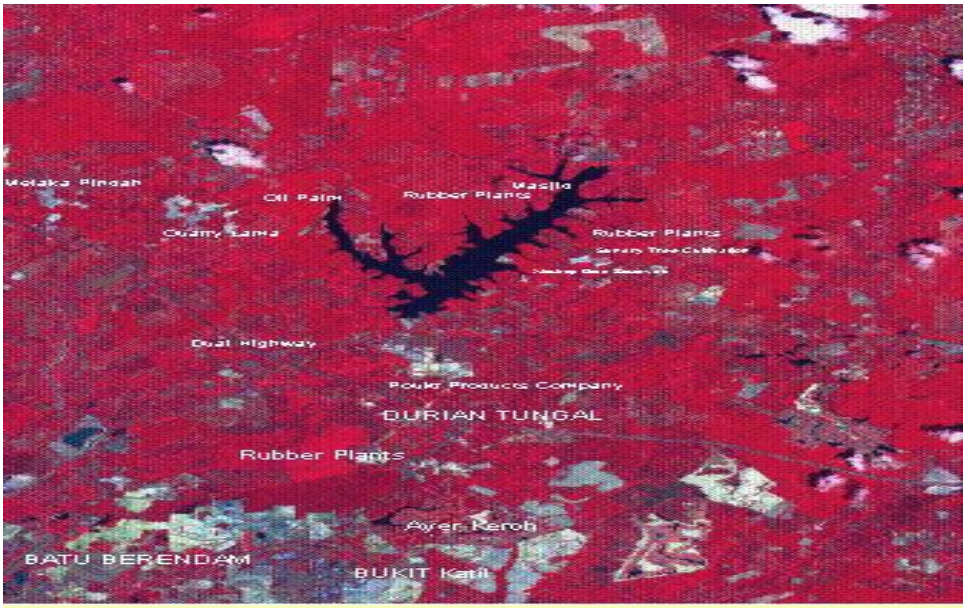

SPOT data of Machap Baru catchment and its surroundings

7

Machap Baru reservoir catchment area

8

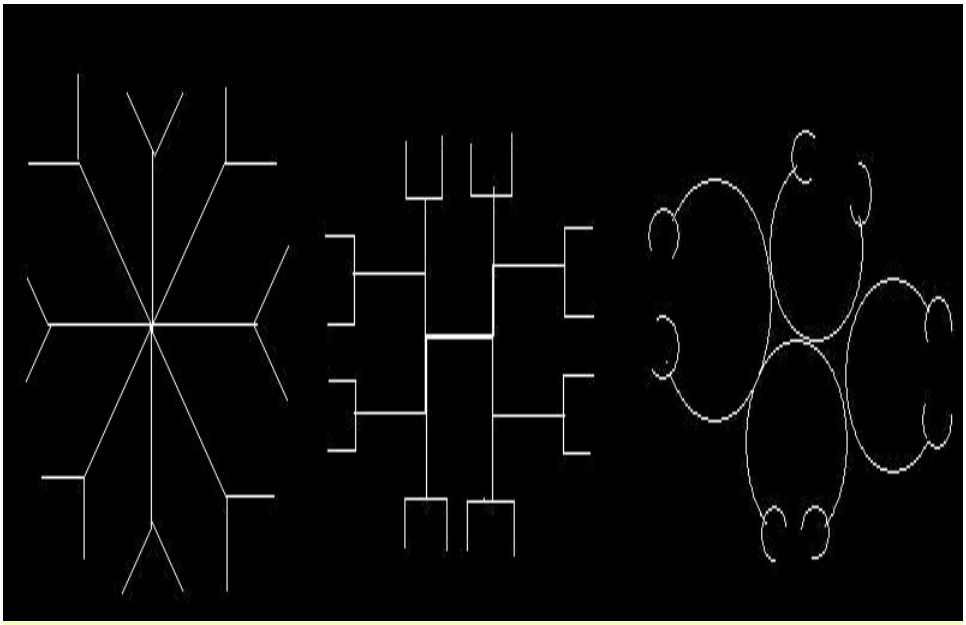

Schematically represented networks 9

Fractal dimension of non-network space of a catchment basin

♦ **Data used:** Stream network of Machap Baru catchment basin traced from topographic map.

♦ **Non-network space:** It is similar to the space that is achieved by subtracting channelized portions from the watershed space.

♦ A technique proposed (i) to generate non-network space of a catchment basin, and (ii) to compute an alternative shape dependent quantity like fractal dimension to characterize the non-network space.

10

Proposed Technique

♦ Step1: Channel network is traced from topographic map.

♦ Step2: Channel network is dilated and eroded iteratively until the entire basin is filled up with white space. This step is to generate catchment boundary automatically. Dilation followed by erosion is called structural closing, which will smoothen the image.

♦ Step3: Generate the basin with channel network and non-network space with boundary by subtracting the channel network from the catchment boundary achieved in Step2.

11

Proposed Technique

♦ Step4: Structural opening (erosion followed by dilation) is performed recursively in basin achieved in Step3 to fill the entire basin of non-network space with varying size of octagons.

♦ Step5: Assign unique color for each size of octagons.

♦ Step6: Compute morphometry for the basin.

♦ Step7: Compute shape dependent dimension.

12

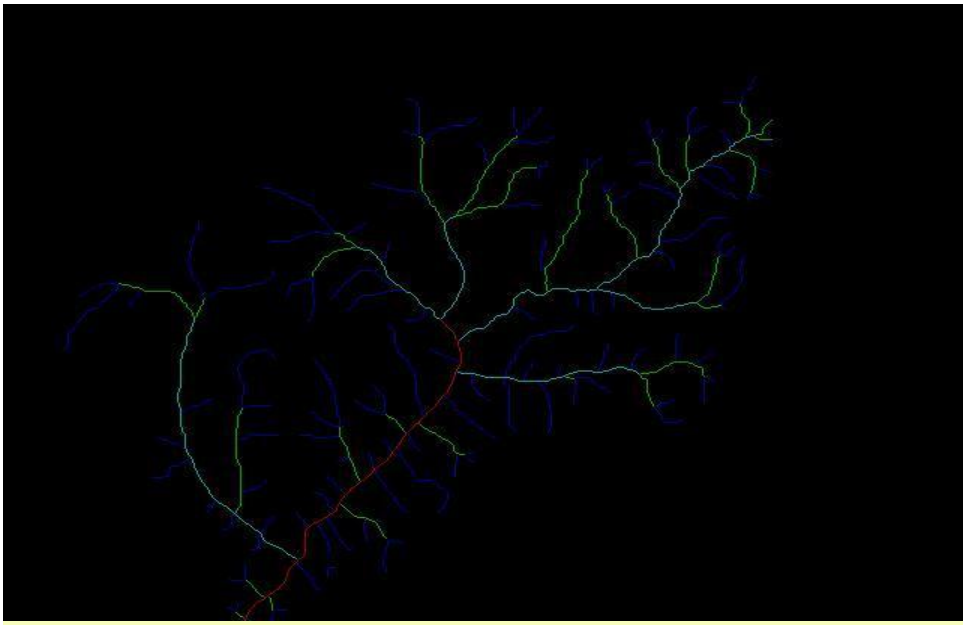

Channel network of Machap Baru reservoir

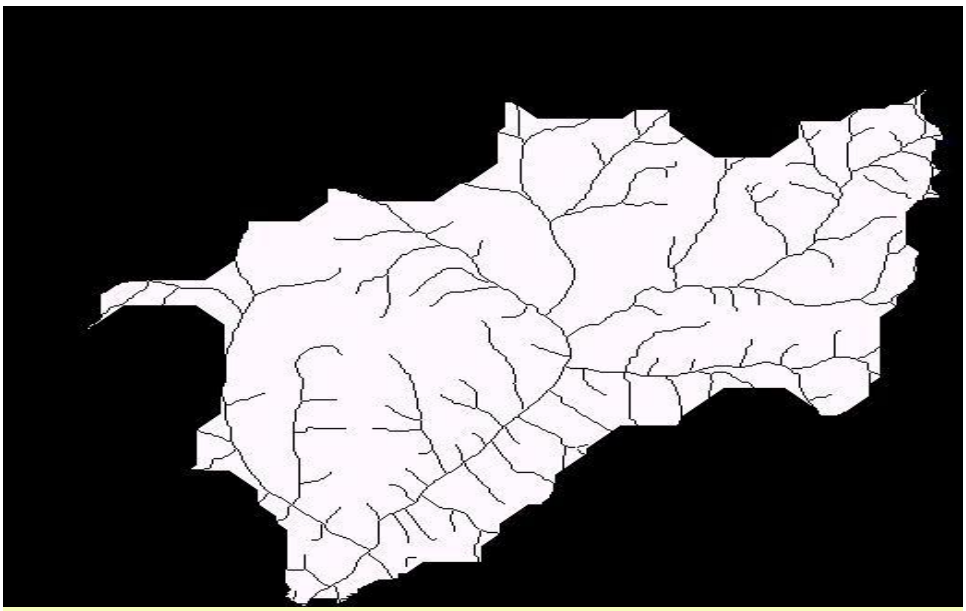

Non-network space within Catchment basin

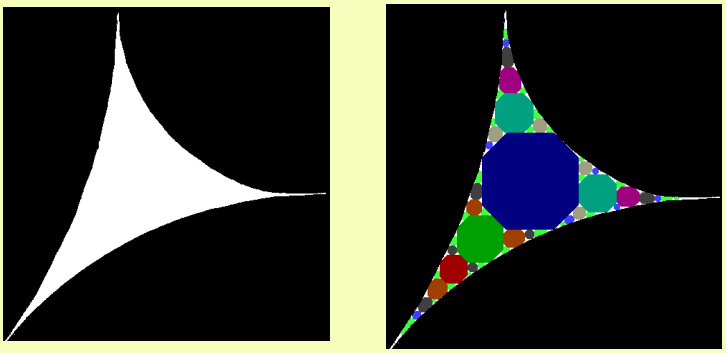

(a) (b)

(a) Appollonian Space, and (b) after decomposition by means of octagon.

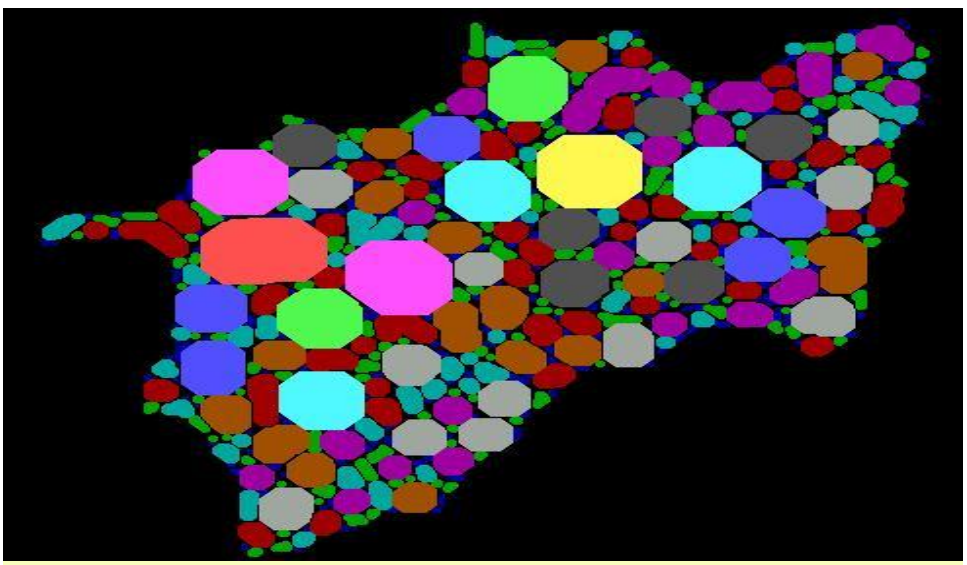

Decomposition of Non-network space in to non-overlapping disks of octagon shape of several sizes

16

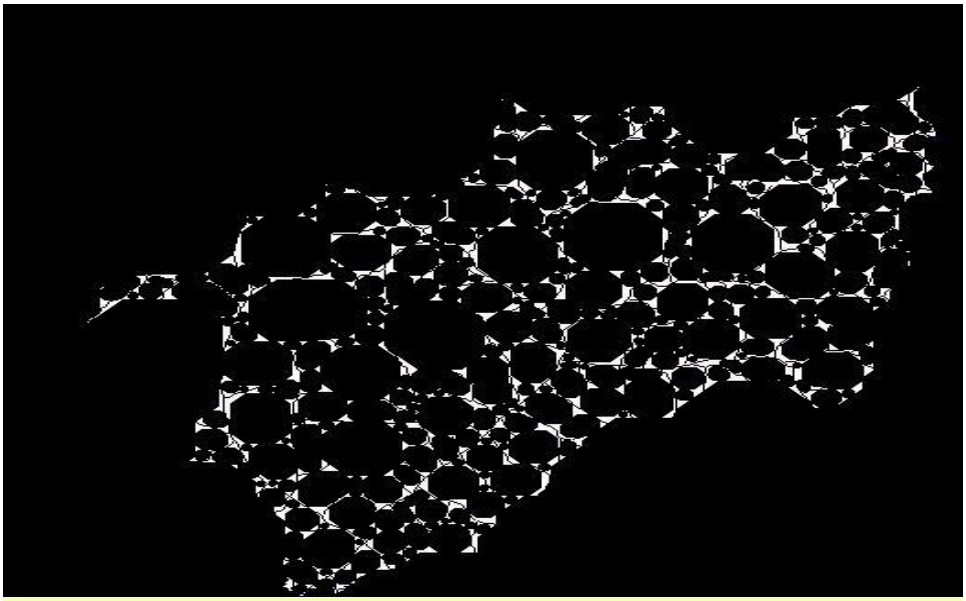

Transition lines between the packed objects

17

Morphometry and shape dependent dimension computation

♦ The ratio of logarithms of bifurcation and mean length ratios of the network yields fractal dimension of 1.77.

♦ Power law exponent is determined for NOD's number and size distributions.

♦ Number of NODs smaller than the specified threshold radius of structuring template and their contributing areas are computed.

♦ Simple Power law relationship is derived by employing these numbers, their contributing areas and the corresponding radius of template.

18

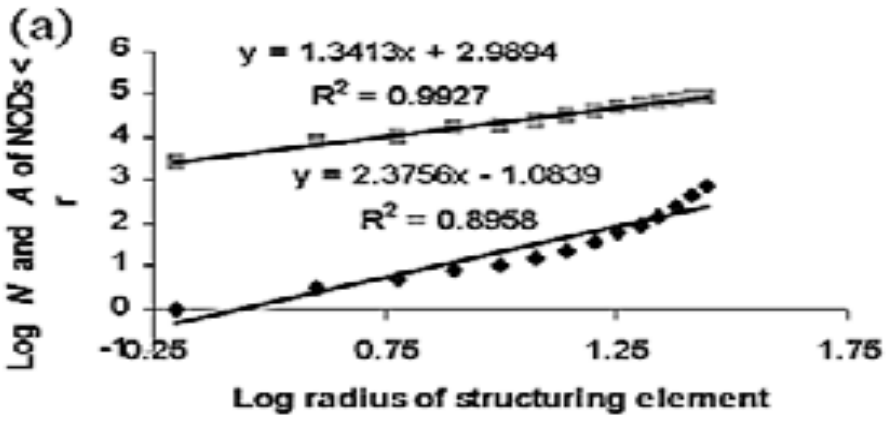

Double logarithmic plot between radii of structuring templates and corresponding number and area of NODs

19

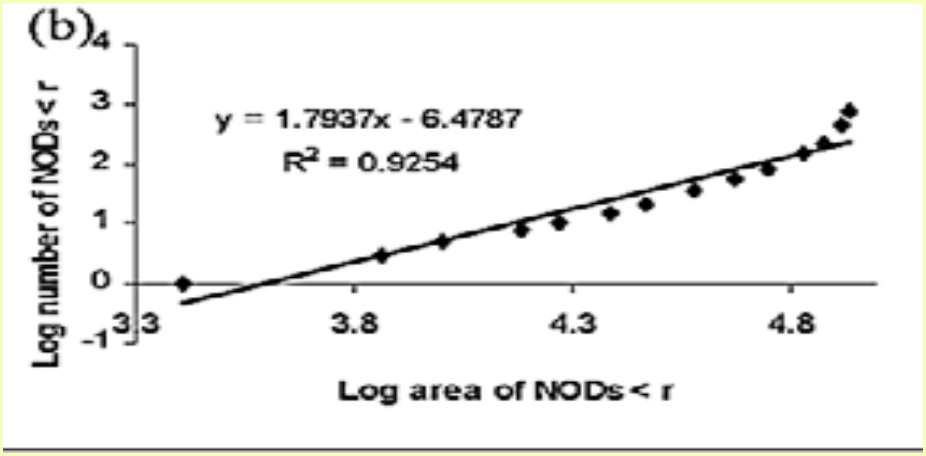

Double logarithmic plot between area and number of NOD's with increasing radius of structuring element

20

Power law relationship

♦ As in previous Fig., the slopes of the best-fit lines (α_N and α_A) for number-radius and area-radius relationships yield 2.37 and 1.34.

♦ These slope values of the best-fit lines provide shape dependent dimensions as $D_N = \alpha_N - 1$ and $D_A = \alpha_A$.

♦ As in previous Fig., D_N and D_A for non-network space yield 1.37 and 1.34.

♦ A Power-law relationship is shown in earlier Fig. with an exponent value 1.79 between the area and number of NODs observed with increasing radius of structuring template

21

Morphometry of Network and Non-Network space

♦ **Data Used:** Digital Elevation Model of Gunung Ledang region.

♦ This technique is adopted to generate non-network space of eight sub-basins of Gunung Ledang region.

♦ In this phase, relationships between the dimensions estimated via morphometries of the network and their corresponding non-network spaces is shown.

22

DEM of Gunung Ledang with 8 sub watershed partition

23

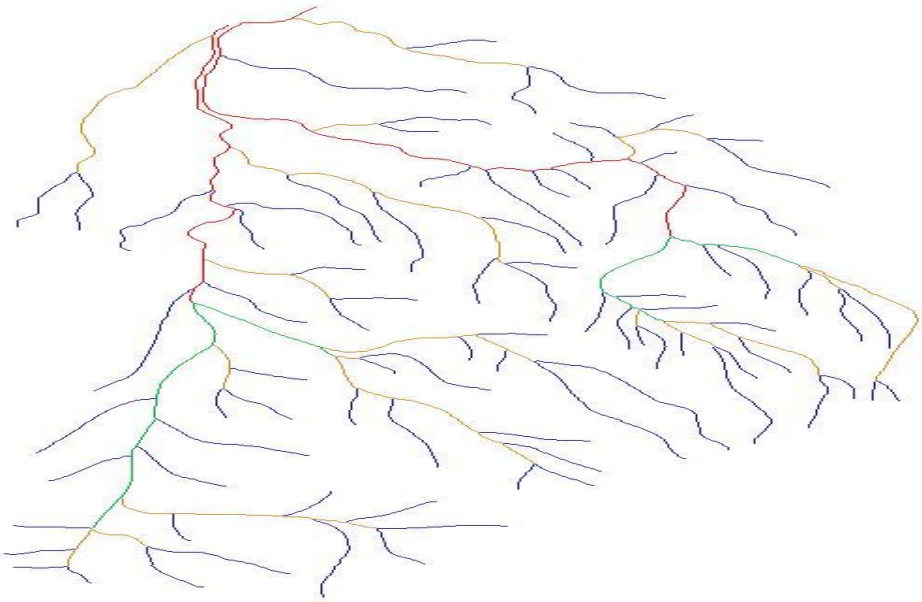

Channel network of sub basin 1

24

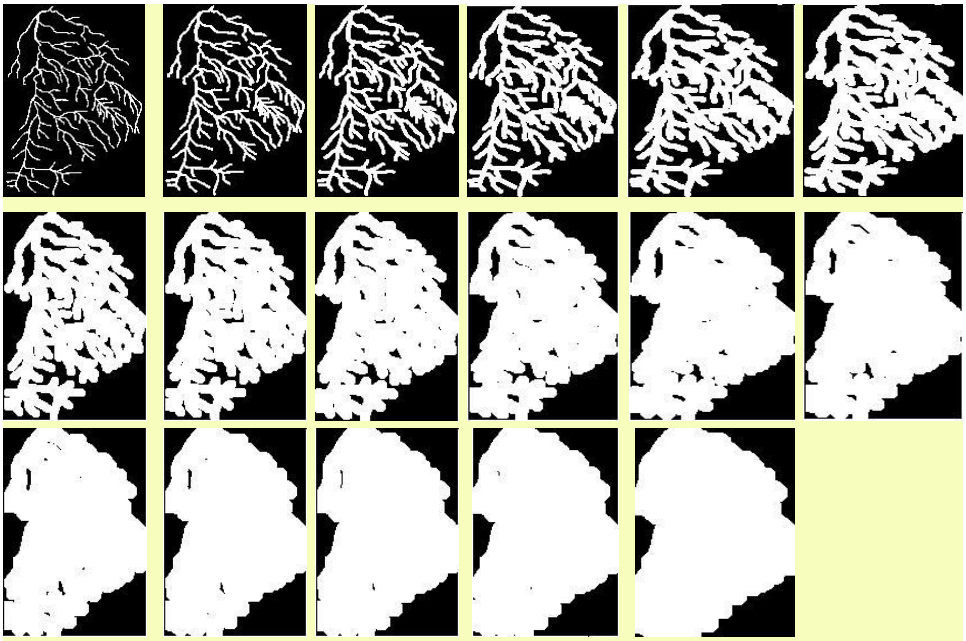

Iterative dilation of channel network of basin 1 25

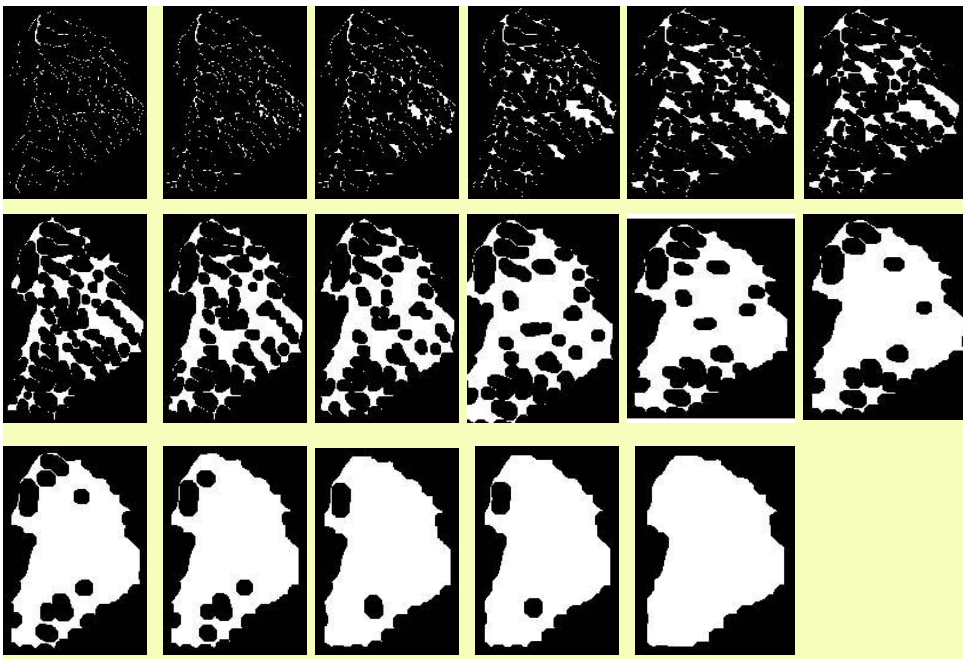

Iterative erosion applied to previous Fig 26

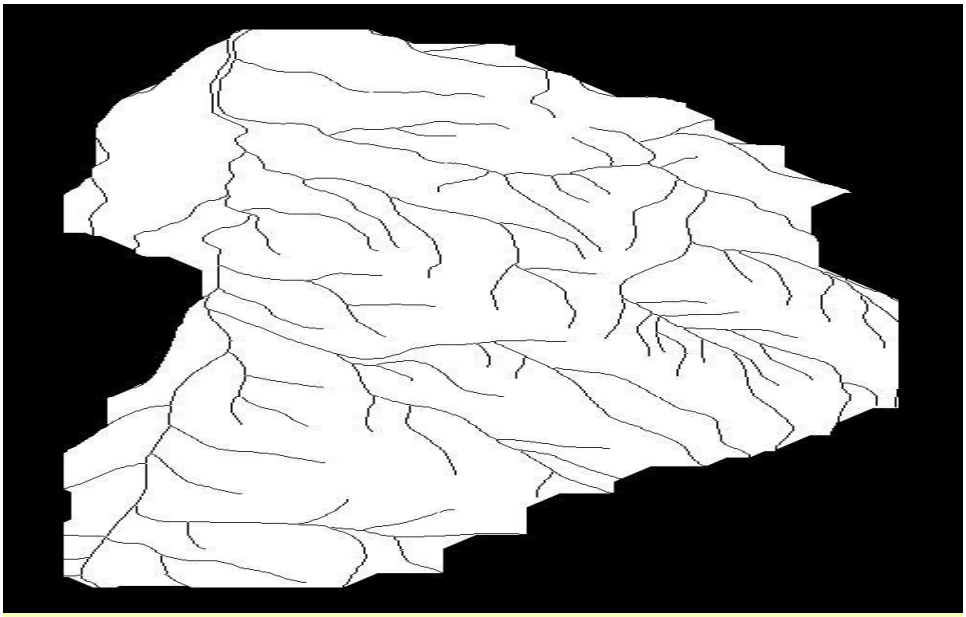

Non-network space of basin 1 27

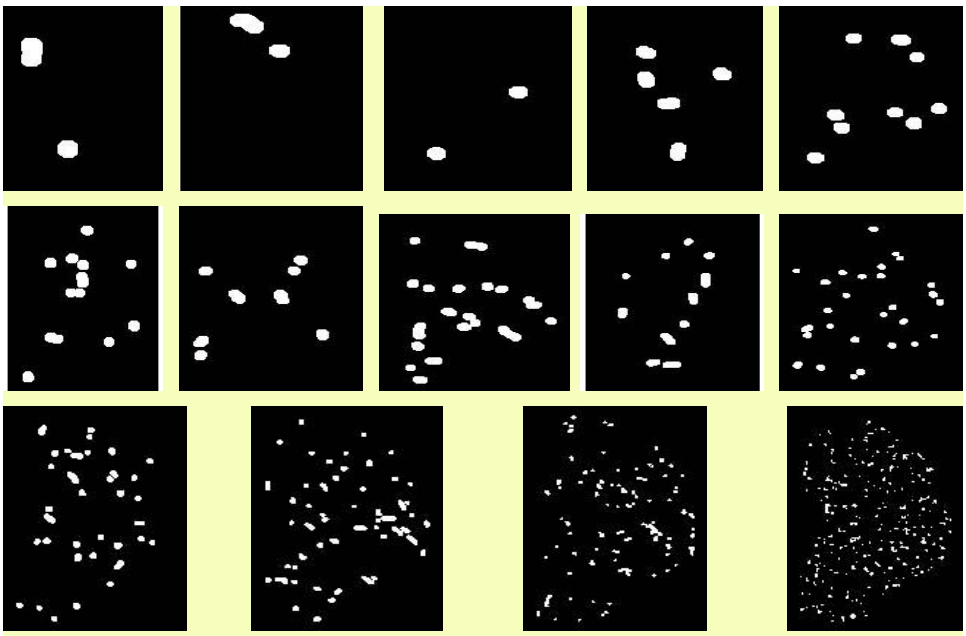

Iterative erosion applied to previous Fig. 28

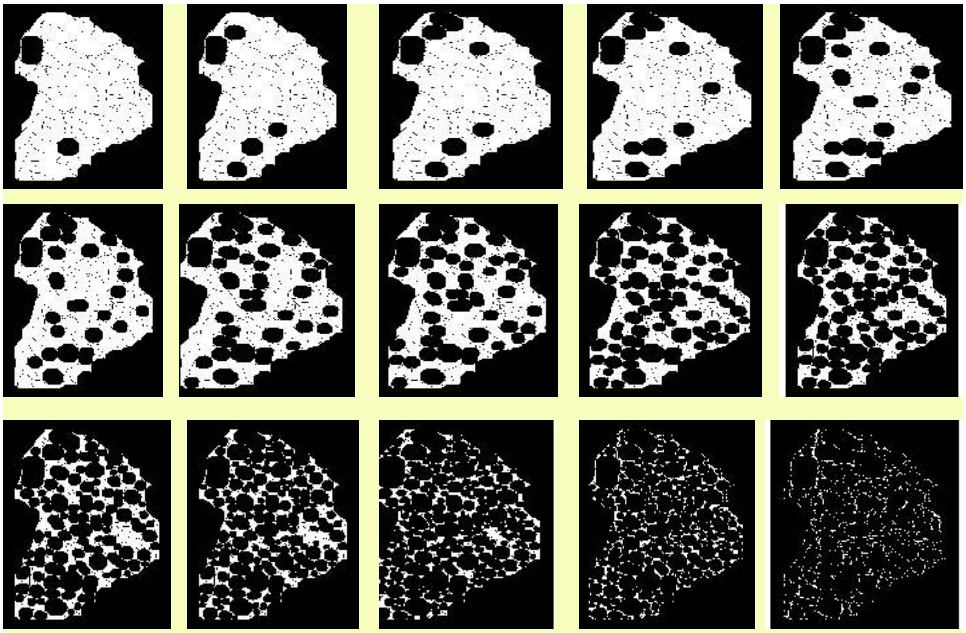

Iterative dilation applied to previous Fig. 29

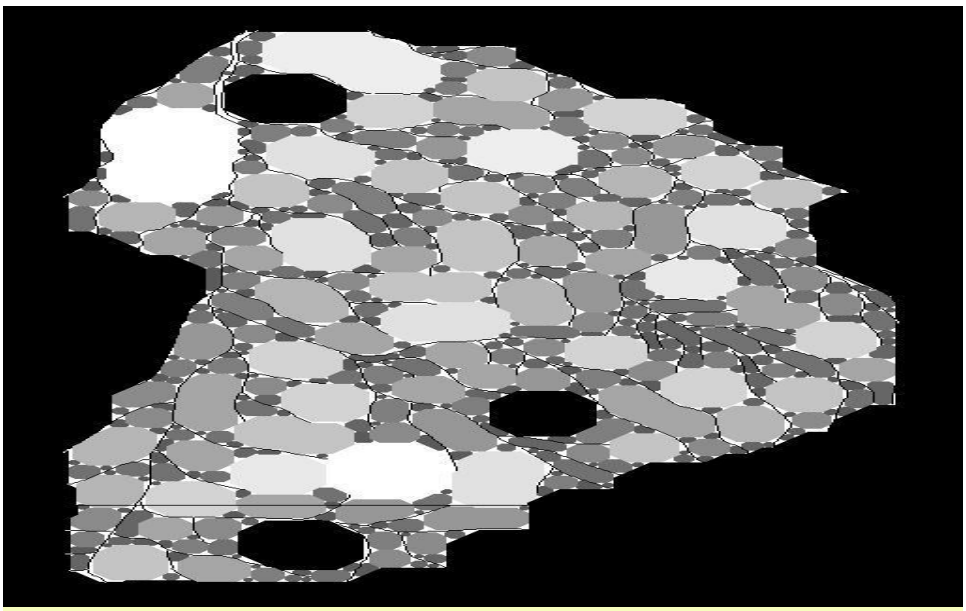

Decomposition of Non-network space in to non-overlapping disks of octagon shape of several sizes for basin 1 30

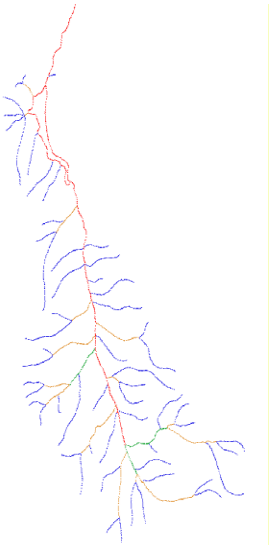
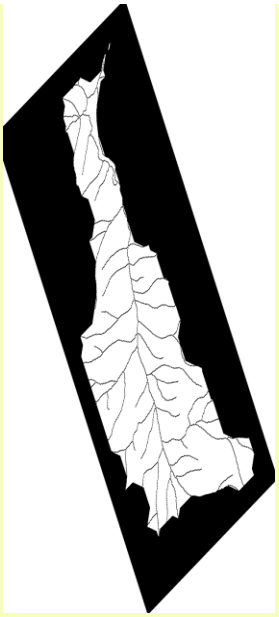
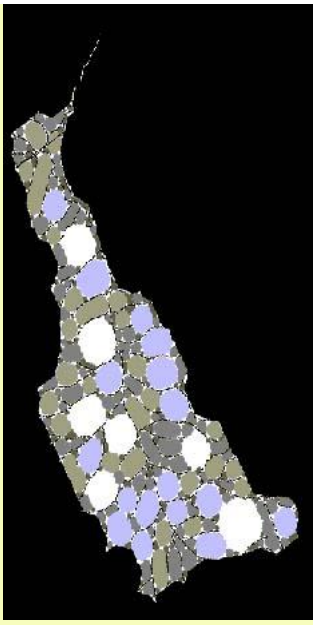

Sub basin 2

31

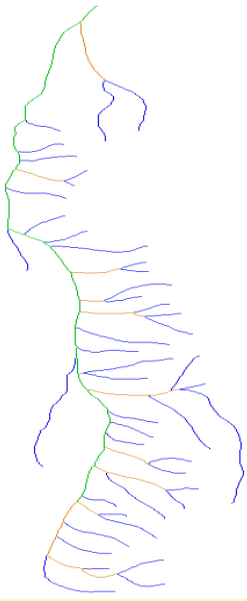
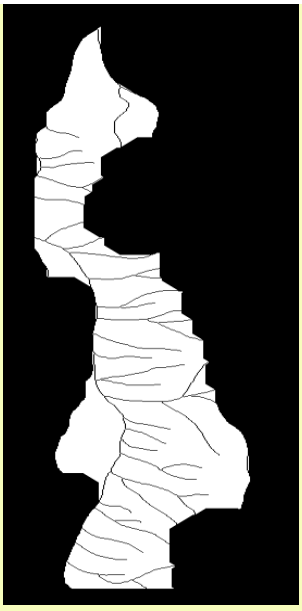
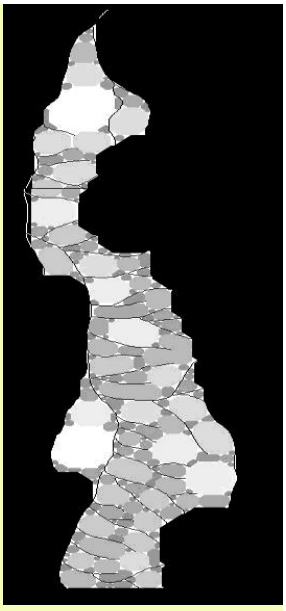

Sub basin 3

32

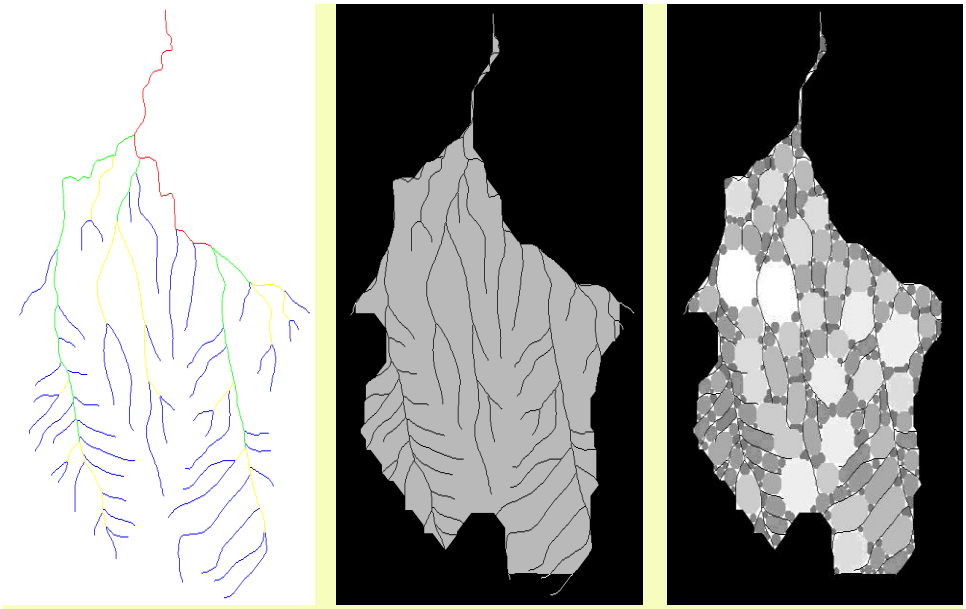

Sub basin 4

33

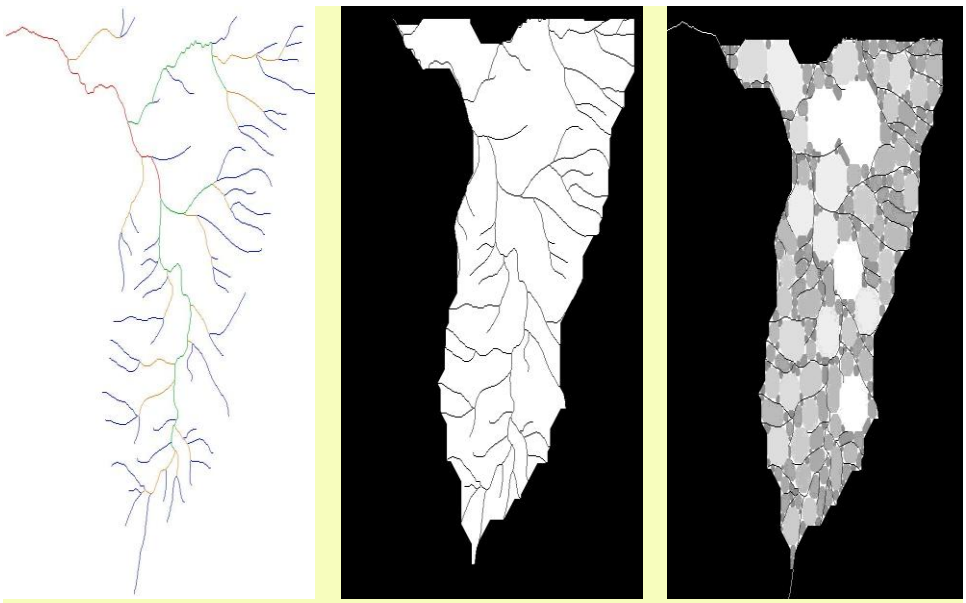

Sub basin 5

34

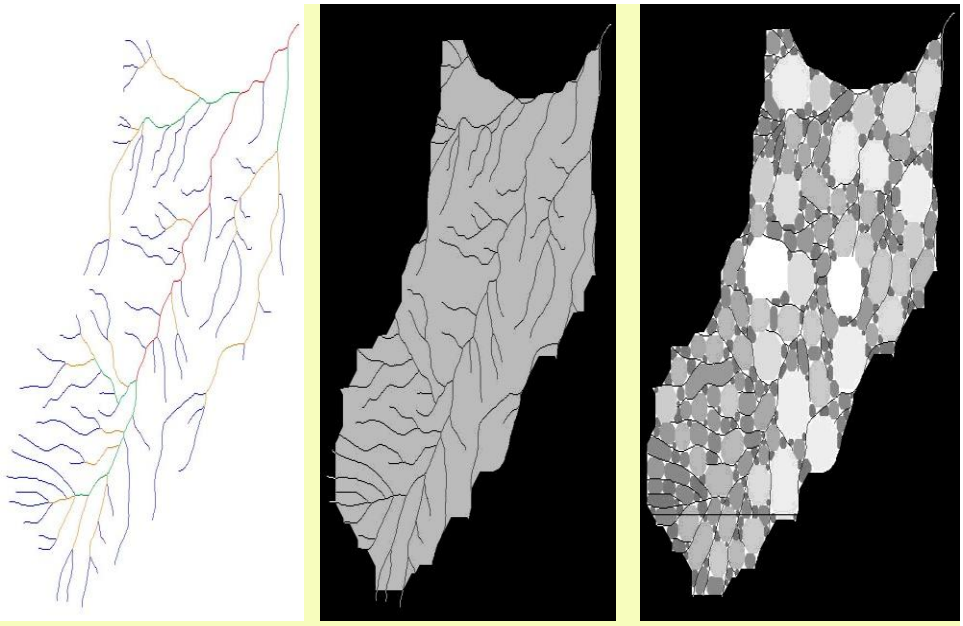

Sub basin 6

35

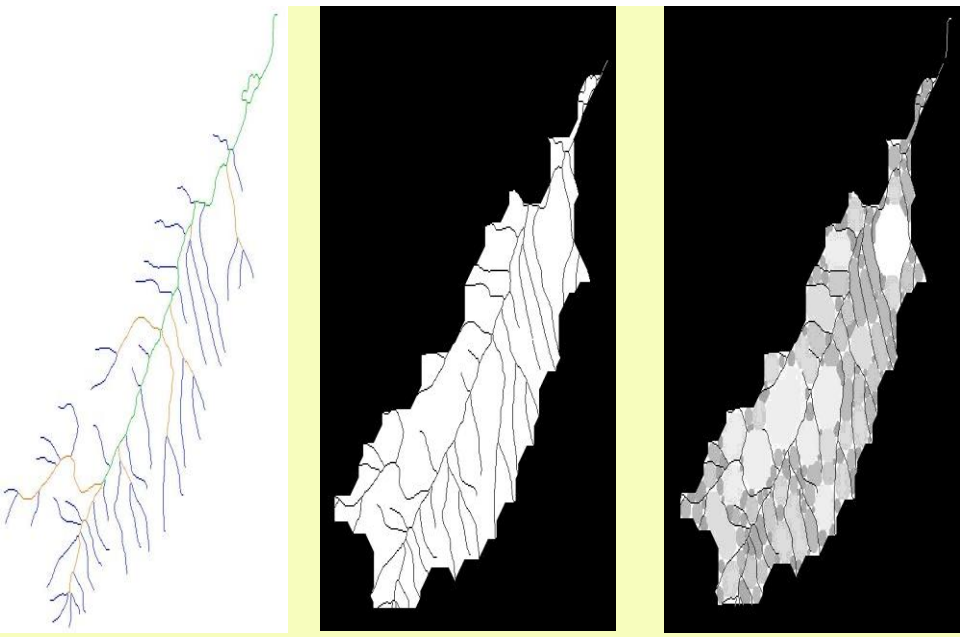

Sub basin 7

36

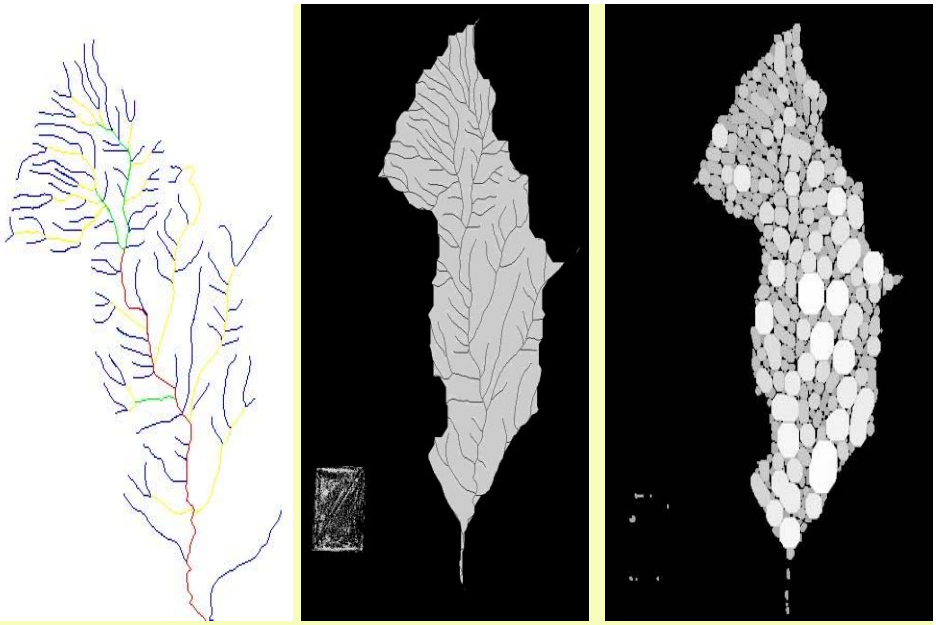

Sub basin 8

37

Basin No	Order Number				Stream length (in pixels)				R_B	R_L
	1	2	3	4	1	2	3	4		
1	85	18	4	2	4891	1611	551	849	3.45	1.90
2	58	15	3	1	2818	775	187	767	3.97	2.33
3	45	11	1	0	2346	594	770	0	6.64	3.87
4	53	11	4	1	2789	748	703	328	3.64	1.90
5	55	17	3	1	2834	961	659	374	3.96	2.07
6	70	18	4	1	3671	1182	518	431	4.16	2.01
7	46	8	1	0	2042	562	479	0	6.78	3.28
8	89	17	3	1	2477	809	194	294	4.57	2.09

Basic measures of networks of eight basins

38

SE	Basin Number															
	1		2		3		4		5		6		7		8	
	N	A	N	A	N	A	N	A	N	A	N	A	N	A	N	A
34	-	-	-	-	-	-	-	-	316	109149	-	-	-	-	-	-
32	520	182014	-	-	-	-	-	-	168	101164	-	-	-	-	-	-
30	273	168813	-	-	-	-	-	-	118	93769	-	-	-	-	-	-
28	273	168813	282	84673	-	-	-	-	118	93769	-	-	-	-	-	-
26	273	168813	143	77373	203	68151	288	91357	77	81823	367	125782	-	-	440	130615
24	185	157455	93	70093	115	63288	152	83715	58	73992	200	116378	179	48876	243	120604
22	132	142011	93	70093	115	63288	104	77487	44	65496	144	108111	100	44098	162	107797
20	97	128123	70	63895	77	57872	77	68878	32	54786	96	94175	68	40018	106	89579
18	69	114338	52	55265	77	57872	58	61020	24	47302	65	80715	41	31764	70	74589
16	58	102690	33	42182	58	53641	40	50716	17	39672	52	72943	41	31764	46	58422
14	39	79374	24	35485	45	48404	28	39683	13	33652	34	58100	26	25760	34	49679
12	31	67158	17	27707	31	38240	17	28488	10	27837	22	45704	13	17946	22	37938
10	20	48742	10	19564	19	28316	10	20138	8	23638	17	40300	9	13669	11	21426
8	11	32274	7	14762	12	20895	7	15941	6	19163	14	36029	5	9833	8	16888
6	6	18356	4	9486	8	16249	5	12226	4	12004	10	28786	4	8888	4	10145
4	4	14019	2	5784	3	8794	2	5587	2	6088	6	16009	2	5435	2	6078
2	2	5859	1	3339	2	6711	1	2753	1	2407	2	5978	1	2360	1	2632

Number & corresponding contributing areas of non-overlapping disks of various sizes decomposed from non-network space of 8 basins

39

Dimensions derived from morphometry of network and non network space

Basin Number	Network FD ($Log R_B / Log R_L$)		R vs A	R vs N	A vs N
1	1.83	193	1.34	2.04	1.50
2	0.86	1.63	1.33	1.23	1.59
3	0.98	1.41	1.02	1.87	1.80
4	2.07	2.01	1.43	2.17	1.52
5	1.73	1.90	1.34	1.94	1.43
6	1.84	2.04	1.13	1.87	1.63
7	1.33	1.61	1.23	2.08	1.70
8	1.65	2.06	1.61	2.38	1.49

40

Graphical plot between stream order and order-wise stream number

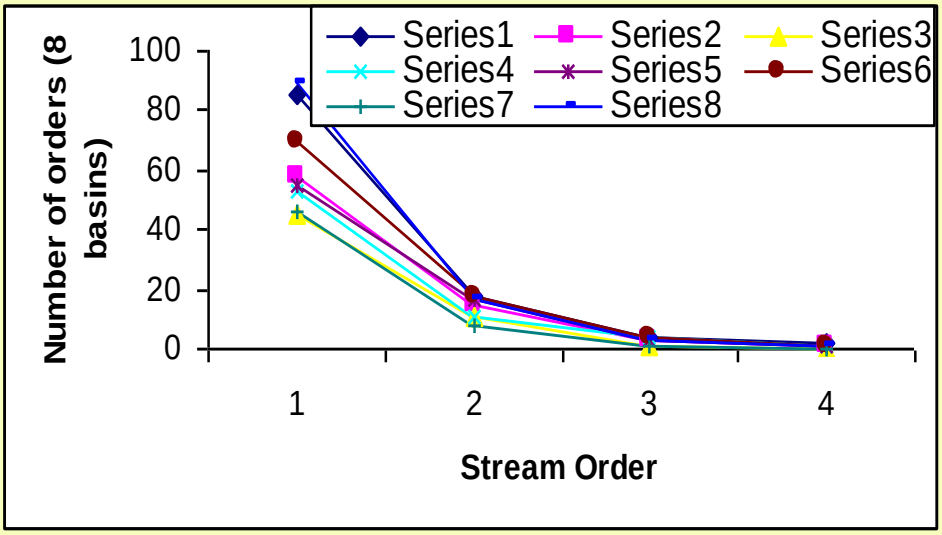

41

Graphical plot between stream order and order-wise stream lengths

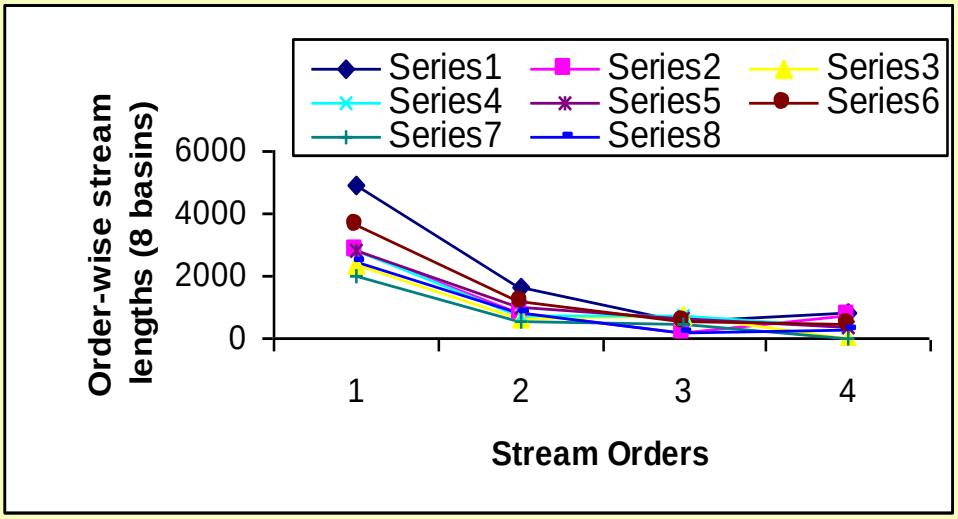

42

Graphical plot between stream order versus logarithm of order-wise numbers for basin 1

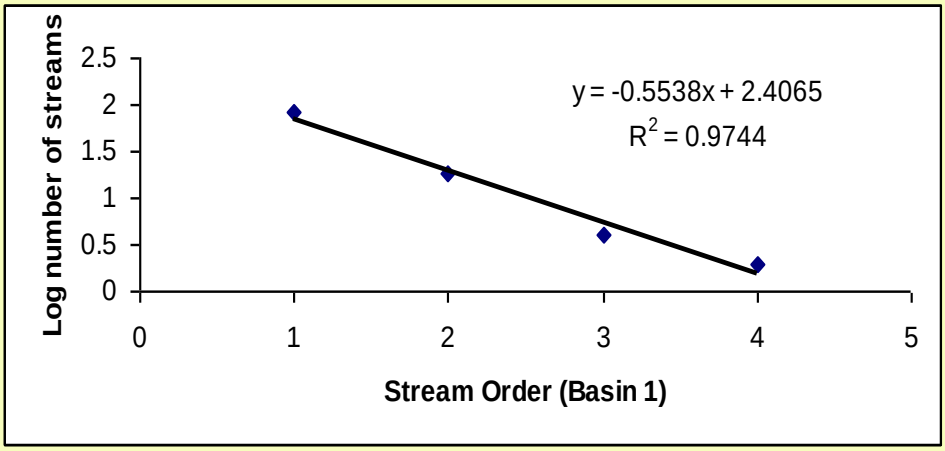

43

Graphical plot between stream order versus order-wise mean stream lengths for basin 1

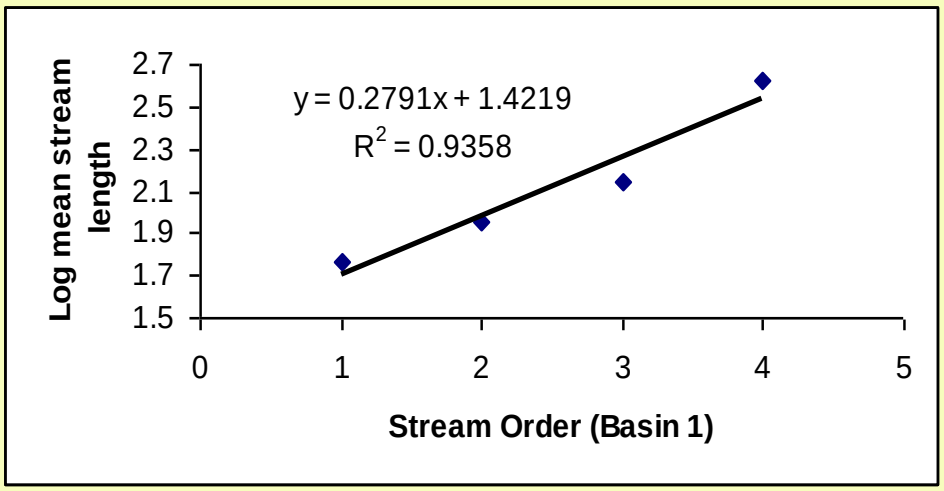

44

Morphometric parameter computations achieved through decomposition of non-network space

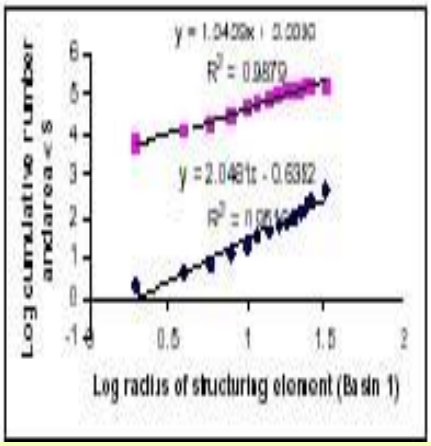

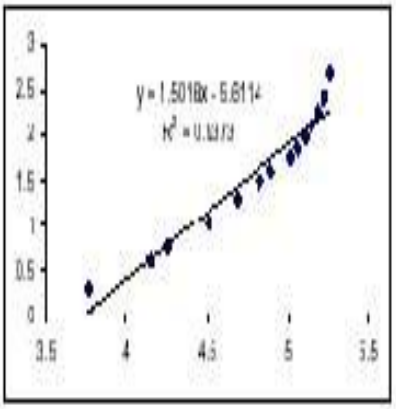

45

Basin number versus varied dimensions derived from morphometry of networks and non-network spaces

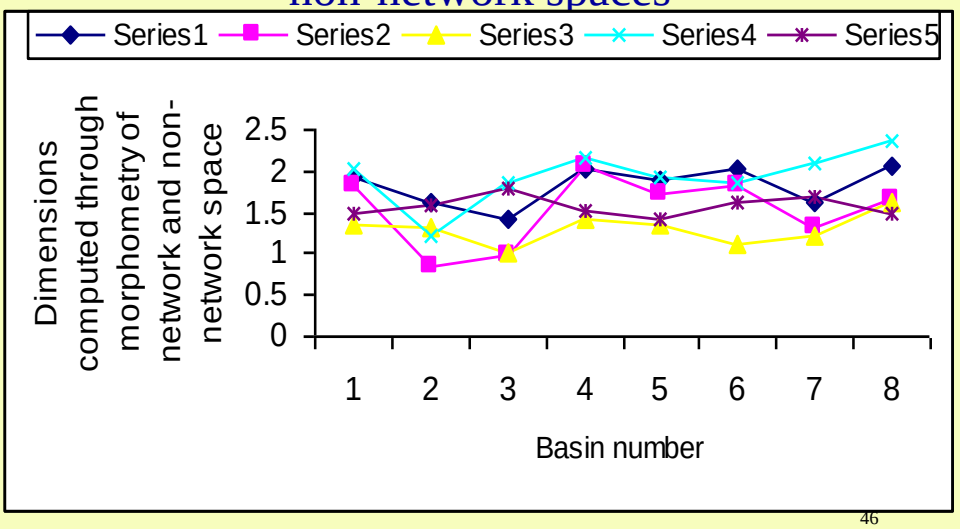

46

Granulometric analysis of digital topography

47

Granulometric analysis

- Morphological multiscaling transformations are shown to be a potential tool in deriving meaningful terrain roughness indices. Resolution constraints is one of the limitations in DEM analyses. In order to overcome these limitations, granulometric approach (a branch of mathematical morphology) is a potential approach because it provides scale-independent surficial roughness indices.
- Consider two different basins of two different physiographic setups (Cameron and Petaling regions) that possess similar topological quantities, their networks may be topologically similar to each other. But the processes involved therein may be highly contrasting due to their different physiographic origins. Under such circumstances, the results that exhibit similarities in terms of topological quantities and scaling exponents would be insufficient to make an appropriate relationship with involved processes.
- Therefore, granulometric approach is proposed to derive shape-size complexity measures of basins. This approach is based on probability distribution functions computed for both protrusions and intrusions (in other words *supremums* and *infimums*) of various degrees of sub-basins.
- This granulometry-based technique is tested on sub-basins with various sizes and shapes decomposed from DEM's of two distinct geomorphic regions, i.e. Cameron Highlands and Petaling region of Peninsular Malaysia.

48

Granulometric analysis

- Multiscale opening till completely black
- Multiscale closing till completely white
- Subtraction

$$PS_f(-n,B) = A[(f \bullet B_n) - (f \bullet B_{n-1})], 1 \le n \le K$$

$$PS_f(+n,B) = A[(f \circ B_n) - (f \circ B_{n+1})], 0 \le n \le N$$

- Probability function

$$ps(n,f) = \frac{A(f \circ B_n) - A(f \circ B_{n+1})}{A(f \circ B_0)}, n = 0,1,2,\ldots,N$$

$$ps(-n,f) = \frac{A(f \bullet B_n) - A(f \bullet B_{n-1})}{A(f \bullet B_K)}, n = 1,2,\ldots,K$$

- Average size

$$AS(f/B) = \sum_{n=0}^{N} n ps(n,f)$$

- Average roughness

$$H(f/B) = -\sum_{k=0}^{n} ps(n,f) \log ps(n,f)$$

Granulometric analysis : Multiscale opening/closing by rhombus

- Scale 1 , 40, 80, 120, 160

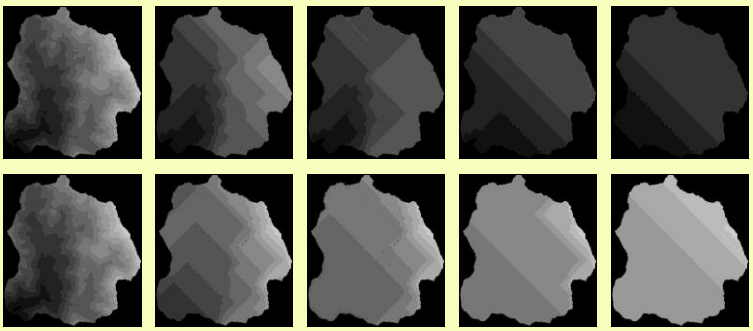

Granulometric analysis :
Multiscale opening/closing by octagon

- Scale 1 , 30, 60, 90, 120

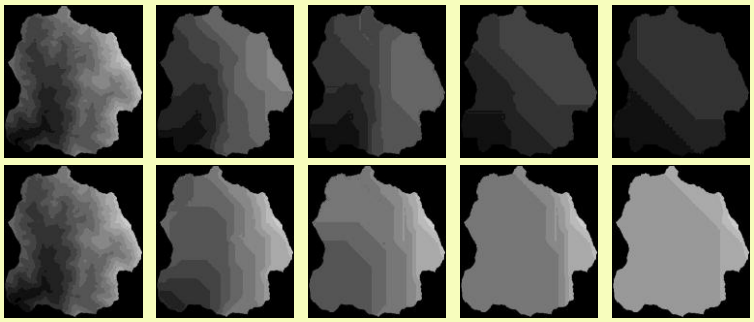

51

Granulometric analysis :
Multiscale opening/closing by square

- Scale 1 , 20, 40, 60, 80

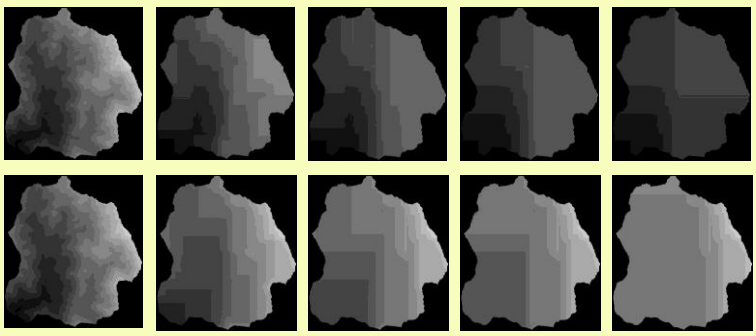

52

Granulometric analysis : Basin wise analysis

- Average size – 14 sub-basins
- Average roughness – 14 sub-basins

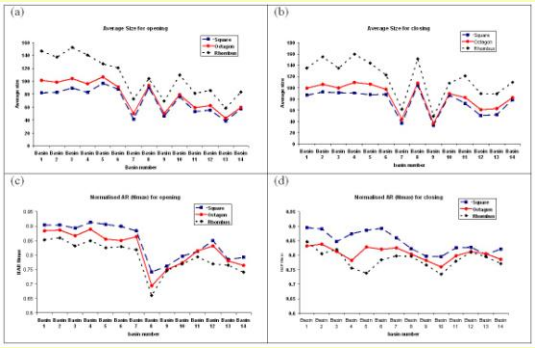

53

Granulometric analysis : Basin wise analysis

- The number of iterations required to make each sub-basin either become darker or brighter depends on the size, shape, origin, orientation of considered primitive template used to perform multiscale openings or closings, and also on the size of the basin and its physiographic composition. More opening/closing cycles are needed when structuring element rhombus is used, and it is followed by octagon and square.
- Mean roughness indicates the shape-content of the basins. If the shape of SE is geometrically similar to basin regions, the average roughness result possesses lower analytical values. If the topography of basin is very different from the shape of SE, high roughness results are produced, which indicate that the basin is rough relative to that SE. In general, all basins are rougher relative to square shape as highest roughness indices are derived when square is used as SE.
- A clear distinction is obvious between the Cameron and Petaling basins. Generally, roughness values of Cameron basins are significantly higher than that of Petaling basins.
- The terrain complexity measures derived granulometrically are scale-independent, but strictly shape-dependent. The shape dependent complexity measures are sensitive to record the variations in basin shape, topology, and geometric organisation of hillslopes.
- Granulometric analysis of basin-wise DEMs is a helpful tool for defining roughness parameters and other morphological/topological quantities.

54

Morphological Complexity Measures

- For surfaces of geophysical nature, complexity measures explain the possible links with the processes involved in the formation of the surface. Such complexity measures include fractal dimension, granulometric indices, fourier descriptors etc.
- Within a surface, there may exist several different regions with different spatial complexities.
- Following the segmented fractal and cloud function, the morphological complexity (also known as roughness indices, or spatial complexity) for each segmented zone is investigated.
- This study offers new insights to quantitative characterization of spatial objects such as trees, and also geophysical fields including clouds, rainfall, temperature, vegetation, elevations, and landscapes.

Data Used

Land Surfaces – Synthetic, Fractal, and Realistic Digital Elevation Models (DEM)

- The synthetic DEM function is a non-negative 2D sequences *f(x,y)*, which assumes $I + 1$ possible intensity values:

  i = 0, 1, 2,…,*I*. Each discrete element with specific numerical value represents elevation at *(x,y)* coordinates.
- As the synthetic Fractal-DEMs deal with 8 bit/pixel digital topographic data, hence $I = 255$.

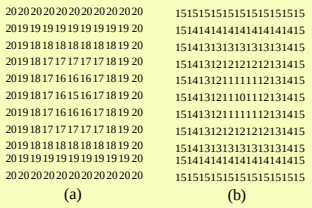

Synthetic DEMs depicted as discrete functions, in which the higher the value the higher is the elevation. In turn these functions are treated as two different DEMs with two different altitudes set-up.

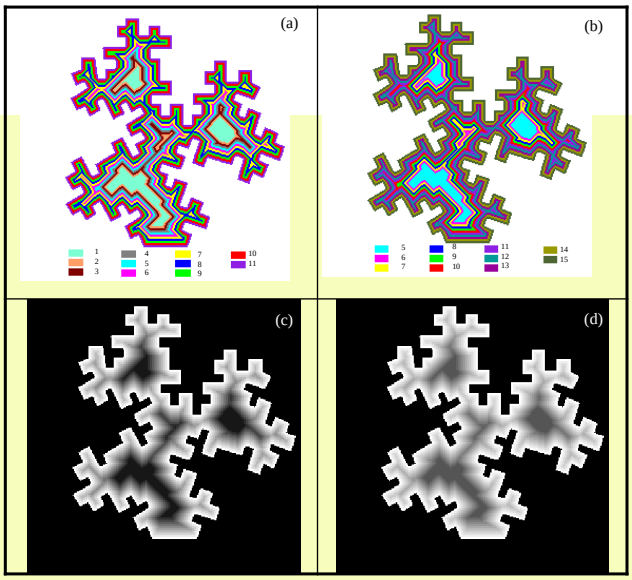

(a, b) Fractal basin functions with elevation ranges of 1-11 and 5-15, (c,d) grayscale versions of fractal functions shown in (a,b).

Function-based Estimation of Drainage Density

- These new approaches are implemented on three types of data: synthetic basin functions, fractal basin functions, and realistic digital elevation models (DEMs) of two regions in Malaysia as basins.
- The results obtained evidently show that the proposed function-based drainage density measures are clearly altitude-dependent which could capture the spatial variability exist within the *homotopic* basins of different altitudes.

Function-based Estimation of Drainage Density

- The three significant parameters which required morphological quantities in the form of functions include (i) basin function itself, (ii) channel network function, and (iii) convex hull of basin function.
- These three functions are respectively denoted as *f(x,y)*, *g(x,y)*, and *CH(f)*.
- The two new ways for estimating the drainage density which mainly based on estimations of length of network and areal aspects of basin and its convex hull are proposed.
- These estimations show distinction on spatial variability between the seemingly alike basins of different altitudes.
- The two possible ways for estimating the drainage density that capture the distinction in terms of spatial variability include (i) ratio between the length of channel network function *A(g)* and the area of basin function *A(f)*, and (ii) ratio between the area of basin function *A(f)* and the area of its corresponding convex hull *A[CH(f)]*.

Function-based Estimation of Drainage Density

- In the basin function, each discrete element with specific numerical value represents elevation at *(x,y)* coordinates.
- DEM is denoted as a function represented by a non-negative 2-D sequence which assumed possible intensity values: $i = 0, 1, 2, \ldots, I$.
- The proposed methods are implemented with two groups of data, namely synthetic DEMs and realistic DEMs. Two types of synthetic DEMs are studied, including simple synthetic functions and fractal basin functions.
- For realistic DEMs, the interferometrically derived topographic synthetic aperture radar (TOPSAR) DEMs of Cameron Highlands and Petaling regions of Malaysia from Tay *et al*. (2007) are used here.

Function-based Estimation of Drainage Density [5/17]

- Various methods exist to derive the channel networks from DEMs in planar forms (O'Callaghan and Mark, 1984; Jenson and Domingue, 1988; Tarboton *et al*., 1991; Band, 1993; Sagar *et al*. 2000).
- For instance, the channel network, shown in next slide, is isolated from DEM via

  (i) threshold decomposition of basin function into threshold elevation sets,

  (ii) isolation of channel subsets through skeletonization operations from threshold elevation sets,

  (iii) subtraction of channel subsets from immediate higher level threshold elevation sets, and

  (iv) composition of channel subsets obtained at step (iii) is superposed on the basin function to perform maximum ($\vee$) operation between the network (subsets derived in the form of a planar set) and their corresponding points from the basin function. Such maxima form the network function.

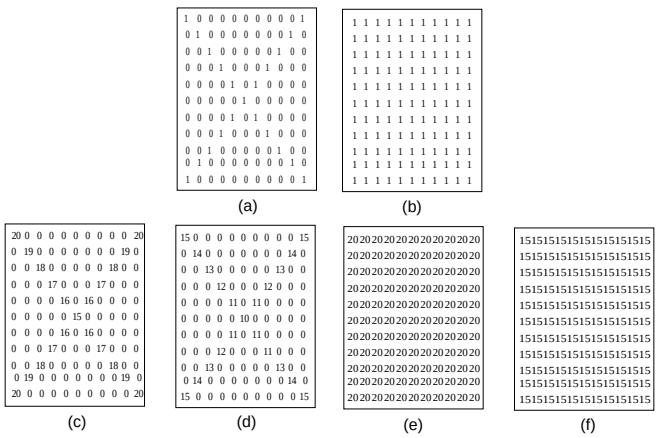

(a) typical planar form of drainage network that summarizes the connectivity and shape of these two functions. It is extracted by following morphology based transformations (Sagar *et al*., 2000). 1s are channel subsets and 0s represent non-channel regions, (b) planar form of the basin areas of the two synthetic basin functions, threshold value employed is <20 and <15 (respectively for two functions shown earlier) and converted into 1s, and 0s for other value(s), (c, d) the elevation values from basin functions shown earlier corresponding to the channel subsets shown in (a), and (e, f) convex hulls of the two synthetic basin functions constructed according to a procedure due to Soille (1998).

Function-based Estimation of Drainage Density

- For discrete basin functions f_1 and f_2 shown earlier and their computed convex hulls.
- The areas under these functions are estimated as
- $A(f) = \sum_{(x,y)} f(x,y)$

  $A(g) = \sum_{(x,y)} g(x,y)$

  $A(CH) = \sum_{(x,y)} CH[f(x,y)]$

  $A(CH) > A(f) > A(g)$
- The areas of these three morphologically significant functions are evidently elevation dependent and hence they are more appropriate to be used in estimating modified drainage density that can capture the basic spatial variability between the basins of different altitudes.
- This is unlike the Hortonian drainage density computation which does not consider the altitudes of the DEMs and thus show similar result for *homotopic* DEMs with different heights,

Function-based Estimation of Drainage Density

- Two approaches are considered - the ratio between (i) areas of channel network and its basin function, and (ii) areas of basin function and its convex hull function:

  (i) $DD_f = \frac{A(g)}{A(f)}$ (method-1) (ii) $DD_f = \frac{A(f)}{A(CH)}$ (method-2)
- These modified drainage densities provide new insights to further explore links with various established and to be derived parameterized morphometric measures in the future.

Basin	Areas of planar forms (pixel)		Areas of functions (pixel)			Drainage density		
	Basin	Network	Basin	Network	Convex hull	Horton-DD	Method-1	Method-2
Function f_1	121	21	2255	375	2420	0.1736	0.1663	0.932
Function f_2	121	21	1650	270	1815	0.1736	0.1636	0.909
Function f_3	20334	1838	152844	12132	396814	0.0904	0.0794	0.3852
Function f_4	20334	1838	234180	19484	541110	0.0904	0.0832	0.4328

Drainage density comparisons for synthetic DEMs.

Function-based Estimation of Drainage Density

- Although both basins have similar geometrical arrangement, basin f_1 has higher elevation than basin f_2: 15 to 20 vs 10 to 15.
- In flat surface form, the area for both basins is the same, which is 121.
- Thus, the Hortonian-DD is also the same: 0.1736.
- If method-1 is applied, the DD is computed as 0.1663 and 0.1636, while method-2 yields 0.9318 and 0.9091, respectively.
- Hence, the drainage densities estimated according to the two proposed methods clearly exhibit spatial variability of the basins, especially those *homotopically* similar basins with different altitude-ranges.

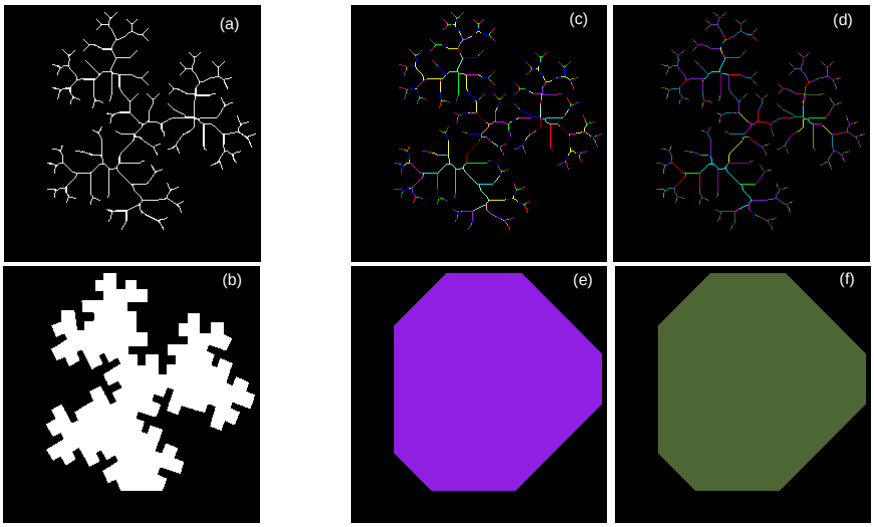

(a) Planar view of the network that represents channel network from both fractal basin functions, (b) planar view of the threshold basin region of both fractal functions, (c, d) channel network functions of the two fractal basin functions, and (e, f) convex hull functions of the two fractal functions.

Function-based Estimation of Drainage Density

- The lengths of planar networks and also areas of plane-view of these two functions are found to be the same.
- As a result, the Hortonian-DD computed for f_3 and f_4 are the same, which is 0.0904, although they exhibit different altitude-ranges.
- As shown in Table, the drainage densities are 0.0794 and 0.0832, 0.3852 and 0.4328 from proposed method-1 and method-2 for fractal basin functions f_3 and f_4, respectively. These drainage densities vary linearly with elevations of the basins. As fractal basin function f_3 has lower altitude range than f_4, its drainage densities computed through method-1 and method-2 are lower than the drainage densities of f_4. Hence, the drainage densities estimated according to the two proposed methods clearly exhibit spatial variability of the basins, especially those *homotopically* similar basins with different altitude-ranges.

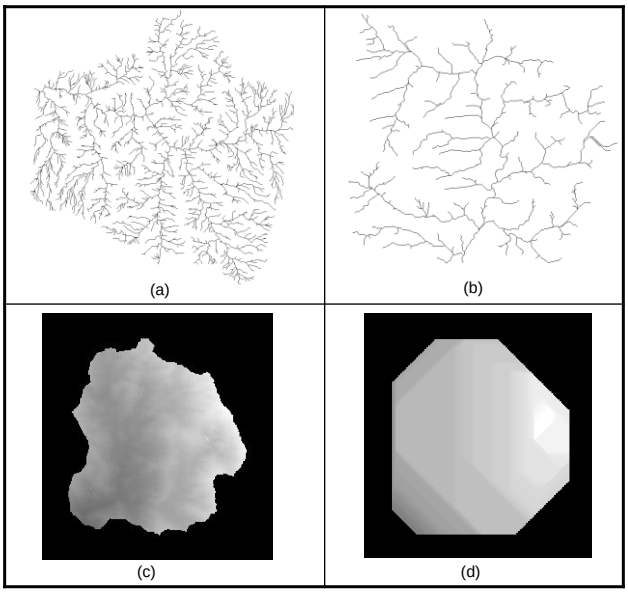

(a) Stream networks extracted from Cameron Highlands DEM, (b) stream networks extracted from Petaling DEM, (c) grayscale DEM of basin 1, and (d) convex hull of basin 1.

Basin	Areas of planar forms (pixel)		Areas of functions (pixel)			Drainage density			Norm complex measure	Fractal dimens
	Basin	Network	Basin	Network	Convex hull	Horton -DD	Method -1	Method -2		
1	71045	3826	6029100	3072600	8555800	0.0539	0.0510	0.7047	0.9130	1.5141
2	77780	4612	7390300	4204400	12549000	0.0593	0.0569	0.5889	0.9362	1.5506
3	84699	4775	8349900	4452000	12274000	0.0564	0.0533	0.6803	0.8963	1.5814
4	55912	3227	5086300	2774300	80163000	0.0577	0.0545	0.6345	0.9165	1.4692
5	41253	2583	4391300	2662800	76397000	0.0626	0.0606	0.5748	0.9255	1.4519
6	31226	2101	3047100	1981400	45184000	0.0673	0.0650	0.6744	0.9291	1.4776
7	19780	1156	1426500	772550	20828000	0.0584	0.0542	0.6849	0.9255	1.3192
8	66824	1629	8124200	167870	14854000	0.0244	0.0207	0.5469	0.7413	1.3140
9	25164	588	2605000	46830	5458100	0.0234	0.0180	0.4773	0.7788	1.2398
10	31779	767	3769600	75553	6088900	0.0241	0.0200	0.6191	0.8038	1.2445
11	35805	808	3703100	65298	7216900	0.0226	0.0176	0.5131	0.8134	1.1817
12	36953	884	3798300	62811	7609700	0.0239	0.0165	0.4991	0.8516	1.2946
13	40845	933	3189600	50907	6578400	0.0228	0.0160	0.4849	0.7921	1.1706
14	23497	576	1786700	31969	3268300	0.0245	0.0179	0.5467	0.7951	1.1721

Drainage density comparisons for realistic DEMs. Basins 1-7 represent Cameron Highlands DEMs, while Basins 8-14 are Petaling DEMs.

Function-based Estimation of Drainage Density

- From Table, the Hortonian-DD computed for Cameron basins range from 0.0539 to 0.0673, while for Petaling basins, the range falls within 0.0226 to 0.0245.
- All the 14 sub-basins have different areas in planar view, and generally the Cameron basins have larger basin areas and network areas than Petaling basins.
- Thus, the Hortonian-DD ranges of Cameron basins should be larger than Petaling basins. In fact, the same trend is also observed from the drainage densities obtained from method-1 and method-2.
- Drainage densities computed from method-1 yield the range of 0.051-0.065 and 0.016-0.0207, and from method-2 they exhibit the range of 0.5748-0.7047 and 0.4773-0.6191, for Cameron basins and Petaling basins, respectively.
- The higher the altitude of the basin, the greater the drainage density, and vice versa.

71

Function-based Estimation of Drainage Density

- To have a better view on the relationships among these various parameters, the graphs in Figs. are generated.
- From these graphs, it is observed that Cameron basins which have higher altitude basins than low-lying Petaling basins, exhibit higher drainage densities (regardless of Horton, method-1, or method-2), higher normalized complexity measures, and also higher fractal dimension values than that of Petaling basins.
- Besides, unlike the case of synthetic basin and fractal basin functions, the drainage densities obtained from method-1 and method-2 for Cameron and Petaling basins correspond well with Horton-DD.
- Furthermore, it is interesting to note from Fig that the drainage density from method-1 follows closely with Horton-DD. Hence, it is conjectured that the proposed method-1 and method-2 offer an alternative way to compute drainage density, which supplements the long-existing Horton-DD.

72

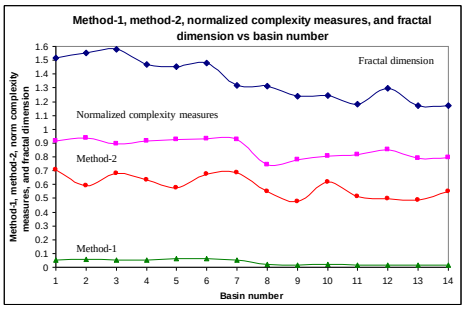

(a)

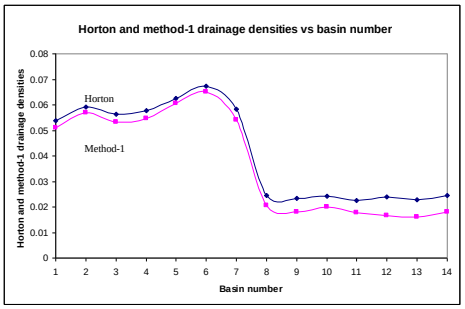

(b)

(a) Drainage densities computed from method-1, method-2, and normalized complexity measures and fractal dimension (via box-counting method) for all 14 basins,

Conclusions

1. Various Computational geophysics related topics are dealt with.

(a) In modeling geophysical phenomena, application of mathematical morphology is relatively less employed. I have addressed several interesting problems by studying the basin via mathematical morphology.

♦ In particular, digital image processing techniques , geo statistical tools and geo computational techniques that are relatively less employed to deal with catchment characterization studies are applied in this investigation.

2. These techniques are proved to be robust in deriving complex topological and surficial features of geophysical significance.

Conclusions

♦ In particular, fragmentation of non-network spaces of several catchment basins of Machap Baru and Gunung Ledang regions is done through a systematic framework.

♦ This framework is primarily based on mathematical morphological transformation.

(b) This framework considers both network topology and geometry of whole basin and non-network space.

♦ Using fragmentation and decomposition rules, significant shape dependent and scale independent topological quantities are derived.

3. These methods and result have outperformed the Strahler-Horton morphometry based network analysis.

75

Acknowledgments: Grateful to collaborators, mentors, reviewers, examiners, and doctoral students—Prof. S. V. L. N. Rao, Prof. B. S. P. Rao, Dr. M. Venu, Mr. Gandhi, Dr. Srinivas, Dr. Radhakrishnan, Dr. Lea Tien Tay, Dr. Chockalingam, Dr. Lim Sin Liang, Dr. Teo Lay Lian, Prof. Jean Serra, Prof. Gabor Korvin, Prof. Arthur Cracknell, Prof. Deekshatulu, Prof. Philippos Pomonis, Prof. Peter Atkinson, Prof. Hien-Teik Chuah and several others.

76